Seroreactivity against tyrosine phosphatase PTPRN links Type 2 Diabetes and Colorectal Cancer and identifies a Potential diagnostic and Therapeutic Target

Running title: PTPRN links diabetes and colorectal cancer

María Garranzo-Asensio[1,2,^] · Guillermo Solís-Fernández[2,3,^] · Ana Montero-Calle[2,^] · José Manuel García-Martínez[4] · Maria Carmen Fiuza[5] · Pilar Pallares[6] · Nuria Palacios-Garcia[7] · Custodia García-Jiménez[4] · Ana Guzman-Aranguez[1] · Rodrigo Barderas[2,*]

1 Departamento de Bioquímica y Biología Molecular, Facultad de Óptica y Optometría, Universidad Complutense de Madrid, Madrid 28040, Spain.
2 Chronic Disease Programme, UFIEC, Instituto de Salud Carlos III, Majadahonda 28220, Madrid, Spain.
3 Molecular Imaging and Photonics Division, Chemistry Department, Faculty of Sciences, KU Leuven, Celestijnenlaan 200F, 3001 Heverlee, Leuven, Belgium
4 Area of Physiology. Dept. CBS, Faculty of Health Sciences, University Rey Juan Carlos, Alcorcon 28922, Madrid, Spain.
5 Surgery Dept. University Hospital Fundación Alcorcon, Alcorcón 28922, Madrid, Spain.
6 Central Units, Instituto de Salud Carlos III, Majadahonda 28220, Madrid, Spain
7 Endocrinology Department, Hospital Universitario Puerta de Hierro, 28222, Madrid, Spain

^These authors contributed equally

*To whom correspondence should be addressed:

Rodrigo Barderas.

Functional Proteomics Unit, UFIEC, Chronic Disease Programme, Instituto de Salud Carlos III, E-28220 Majadahonda, Madrid, Spain; Tel.: 34-91-8223231; E-mail: r.barderasm@isciii.es

Word count:	5146
Tables:	1
Figures:	6
Supplementary Files:	3 (2 tables and supplementary material).

Twitter: @ProteoFun

Tweet: New research shows that seroreactivity against PTPRN links type 2 diabetes with colorectal cancer, identifying PTPRN as a diagnostic and potential therapeutic target in colorectal cancer @ProteoFun @SaludISCIII

(Figure 6 summarizes PTPRN potential as therapeutic target)

ABSTRACT

Colorectal cancer (CRC) and diabetes are two of the most prevalent chronic diseases worldwide with dysregulated receptor tyrosine kinase signaling and strong co-occurrence correlation. Plasma autoantibodies represent a promising early diagnostic marker for both diseases before symptoms appear. We explore here the value of autoantibodies against receptor-type tyrosine-protein phosphatase-like N PTPRN (full-length or selected domains) as diagnostic markers using a cohort of type 2 diabetic (T2D), CRC, healthy individuals or patients with both diseases. We show that PTPRN autoantibody levels in plasma discriminated between T2D patients with and without CRC. Consistently, high PTPRN expression correlated with decreased survival of CRC patients. Mechanistically, PTPRN depletion significantly reduced invasiveness of CRC cells *in vitro* and liver homing and metastasis *in vivo* by means of a dysregulation of the epithelial-mesenchymal transition and a decrease of the insulin receptor signaling pathway. Therefore, PTPRN autoantibodies may represent a particularly helpful marker for the stratification of T2D patients at high risk of developing CRC. Consistent with the critical role played by tyrosine kinases in diabetes and tumor biology, we provide evidences that tyrosine phosphatases such as PTPRN may hold potential as therapeutic targets in CRC patients.

KEYWORDS: cancer, colorectal cancer, diabetes, diagnostic and therapeutic markers, humoral immune response, PTPRN

INTRODUCTION

Cancer and diabetes are among the most prevalent chronic diseases worldwide. Diabetes encompasses a group of metabolic diseases in which insulin deficiency and/or resistance results in hyperglycemia (1). In type 1 diabetes (T1D), there is an autoimmune destruction of pancreatic β-cells that produces a complete insulin deficiency (1; 2). These patients usually have autoantibodies against insulin, glutamic acid decarboxylase (GAD65), and tyrosine phosphatase-related proteins such as receptor-type tyrosine-protein phosphatase-like N (PTPRN, more commonly known as islet antigen-2 (IA-2)). On the other hand, type 2 diabetes (T2D) is characterized by insulin resistance (1). In contrast with T1D, T2D develops slowly during adulthood as a consequence of insulin resistance with initial hyperinsulinemia to compensate. Insulin receptor belongs to the tyrosine kinase (TK) superfamily and its signaling is altered in both types of diabetes. Constitutively active TK signaling is a hallmark of cancer. TK signaling is switched off by tyrosine-phosphatases which, not surprisingly, are also frequently altered in cancers. The protein family of phosphotyrosine phosphatase receptors (PTPR), with 21 members, is involved in immune regulation, and in vascular and nervous system development (3-6). Although this protein family still remains poorly characterized in cancer, PTPR proteins with oncogenic and tumor suppressor features have been reported in different cancers (7).

PTPRN is a single pass transmembrane protein, found in secretory vesicles and plasma membrane. PTPRN is composed of an extracellular domain (ECD), a single transmembrane region (TM), and an intracellular domain (ICD). Notably, cleaved ICD translocates into the nucleus of beta cells where it induces the expression of the insulin gene through convergence with STAT3 and STAT5 signaling. In addition, PTPRN, which does not have intrinsic phosphatase activity, might regulate tyrosine phosphatase PTPRA through dimerization (8). Aberrant PTPRN expression has been reported in diabetes and in cancer (9; 10). PTPRN is expressed in the pancreatic islets and neuroendocrine cells, suggesting that it plays an important role in hormone and neurotransmitter secretion (11-14). In cancer, PTPRN is considered an unfavorable disease marker for hepatocellular carcinoma and glioblastoma (12; 15). In addition,

PTPRN alterations (mutations, deletions, etc) have been reported in many cancer types. Furthermore, PTPRN hypermethylation and overexpression correlates with increased tumor growth, cellular proliferation and shorter survival in ovarian and small cell lung cancer (13; 16). However, the importance of PTPRN alterations in highly prevalent cancer types, such as colorectal cancer (CRC), remains unknown.

In type 1 diabetes, PTPRN is a common target of autoantibodies, whose levels can be measured to detect and predict the pathology (9). In cancer, autoantibodies are commonly produced against tumor associated antigens well before the clinical symptoms appear (17-21). Therefore, they offer an interesting alternative as disease biomarkers. Thus, cancer related autoantibodies are usually produced against proteins involved in cancer initiation and/or progression, and proteins that modulate the tumorigenic properties of cancer cells (proliferation, invasion, aggressiveness…), which could help narrowing down potential disease markers and therapeutic targets (22). Since T2D patients have an increased CRC risk (after correction for obesity and other confounding factors) compared to the general population (2; 23-25), autoantibodies might serve to identify CRC patients among T2D individuals.

In this work, we have analyzed PTPRN seroreactivity in a well characterized patients cohort composed of healthy individuals, T2D patients, CRC patients and CRC and T2D patients to determine its usefulness to discriminate CRC patients. Interestingly, the seroreactivity analysis was able to significantly discriminate control and diabetic individuals from those with CRC and diabetes, indicating PTPRN seroreactivity could help in the identification of those T2D patients more prone to develop CRC. Furthermore, PTPRN *in vitro* and *in vivo* loss-of-function assays evidenced an important role of PTPRN in the tumorigenic and metastatic properties of CRC cells.

RESEARCH DESIGN AND METHODS

Study Population

Thirty-eight individuals including patients diagnosed with T2D or/and CRC who underwent surgery at Hospital Fundación Alcorcón (HUFA, Alcorcón, Madrid, Spain), and healthy control subjects, were assessed for eligibility according to the following inclusion/exclusion criteria (Table 1 and Supplementary Table 1). Inclusion criteria: patients who: a) underwent surgery to remove visceral fat with type 2 diabetes, b) as previous section but not diabetic, c) were going to undergo surgery to remove a colorectal cancer tumor and are diabetic, or d) same as c) but not diabetic. Recruited patients were divided between the two genders and had comparable body mass index and age. Exclusion criteria: patients who: a) consume large amounts of alcohol or are smokers, b) have papillomavirus or *Helicobacter pylori* infections, c) patients treated with immunosuppressants prior to surgery, d) patients treated with chemotherapy prior to surgery, e) suffer from infectious diseases, f) were receiving radiation therapy, or g) with autoimmune inflammatory pathology, because these conditions may alter per se the presence of tumor markers in blood.

The institutional review board of HUFA evaluated the clinical and ethical aspects of the study, granting approval on June 8th, 2017. All patients gave written informed consent for the use of their biological samples for research purposes. Ethical principles promoted by Spain (LOPD 15/1999) and the European Union Fundamental Rights of the EU (2000/C364/01) were followed. All patients' data were processed according to Declaration of Helsinki (last revision 2013) and Spanish National Biomedical Research Law (14/2007, of 3 July). Blood samples were rapidly processed to obtain plasma fractions and stored at -80ºC until use (19; 26-28).

For the evaluation of PTPRN seroreactivity and its extra- and intra-cellular (ECD and ICD) domains experiments were performed in triplicate. A total of 18 colorectal cancer patients (10 plasma samples from non-diabetic colorectal cancer (CRC) patients and 8 plasma samples from type 2 diabetic CRC patients) and 20 control samples (10 plasma samples from healthy control individuals and 10 plasma samples from type 2 diabetic individuals) were used (Table 1).

Cell Lines

KM12C and KM12SM isogenic CRC cell lines used for the *in vitro* functional cell-based and *in vivo* assays were obtained from I. Fidler's laboratory (MD Anderson Cancer Center). KM12SM cells possess high metastatic capacity to liver, whereas KM12C cells are poorly metastatic (29; 30). KM12SM cells stably expressing firefly luciferase (KM12SM-vLuc cells) were obtained according to established protocols (31).

Cells were grown and maintained in DMEM supplemented with 10% inactivated FBS, L-Glutamine and penicillin/streptomycin at 37ºC and 5% CO_2. Each 15 days cells were monitored for the absence of mycoplasma contamination.

Gateway Plasmid Construction, Gene Cloning, DNA Preparation and Protein Expression

Sequence-verified, full-length cDNA plasmid containing PTPRN, extra- and intra-cellular domains of PTPRN and HaloTag protein were obtained either from the publicly available DNASU Plasmid Repository (https://dnasu.org/DNASU/) or by PCR using specific primers (Supplementary Table 2 and Supplementary Material) (32-34).

SDS-PAGE and Western Blot Analysis

SDS-PAGE and western blot analysis to assess protein quality was performed as previously reported (34; 35). Briefly, 0.67 µl of the *in vitro* protein extracts or 10 µg of KM12C and KM12SM protein extracts were separated in 10% SDS-PAGE and transferred to nitrocellulose membranes (Hybond-C extra). After blocking, membranes were incubated overnight at 4 °C with an anti-HaloTag monoclonal antibody (Promega, #6921A) diluted 1:1000, an anti-PTPRN monoclonal antibody (SCBT, sc-130570) diluted 1:200, an anti-p-insulin Rβ polyclonal antibody (SCBT, sc-25103-R) diluted 1:1000, an anti-IRS1 polyclonal antibody (SCBT, sc-559) diluted 1:1000, an anti-p-FOXO1/3 polyclonal antibody (Cell Signaling, #9464), an anti-AKT polyclonal antibody (Cell Signaling Technology, #4691), an anti-pAKT polyclonal antibody (Cell Signaling Technology, #9275), an anti-ERK polyclonal antibody (Cell Signaling Technology, #4695), an anti-pERK polyclonal antibody (Cell Signaling Technology, #9101), an

anti-GSK3β monoclonal antibody (BD Transduction Laboratories, #61021), an anti-GAPDH (Rockland, 800-656-7625) diluted 1:2000 or an anti-RhoGDi (SCBT, sc-360) diluted 1:1000. Immunodetection on nitrocellulose membranes was achieved by using HRP-conjugated goat anti-mouse IgG antibody or HRP-conjugated goat anti-rabbit IgG antibody (Sigma). Chemiluminescence signal was developed with ECL Western Blotting Substrate (Thermo Fisher Scientific) and detected on an Amersham Imager 680 (GE Healthcare).

Bioinformatic Analysis

Meta-analysis information regarding PTPRN genetic and protein expression levels in CRC were retrieved from the cBioPortal (https://www.cbioportal.org/) and Oncomine (https://www.oncomine.org/). Survival analyses were performed using the GEPIA2 web server (http://gepia2.cancer-pku.cn/#index), and colon adenocarcinoma (COAD) and/or rectal adenocarcinoma (READ) TCGA (The Cancer Genome Atlas) datasets.

EBNA1 ELISA and PTPRN Luminescence Beads Seroreactive Immunoassay

Colorimetric ELISA for EBNA1 antibody determination for the evaluation of the specificity of the study was achieved coating 0.05 µg of EBNA1 protein (kindly provided by Protein Alternatives, S.L.) per well in 50 µl of phosphate-buffer saline solution (PBS) in 96-well transparent plates (Nunc) overnight at 4ºC according to established protocols (32; 34; 36).

PTPRN luminescence beads seroreactive immunoassay was performed according to established protocols (32; 34). See Supplementary Material for information in detail.

Transient PTPRN Silencing

For transient PTPRN silencing, transfection was performed in 6 well-plates using the jetPRIME reactive (PolyPlus Transfection) with, alternatively, three siRNAs targeting PTPRN to account for potential off-target effect (PTPRN #1 (SIHP0814-SIHP0816; Sigma Aldrich), PTPRN #2 (EHU029231; Sigma-Aldrich), PTPRN #3 (sc-62902; SCBT)) or control siRNAs (SIC001; Sigma-Aldrich) following the manufacturer's instructions. Briefly, $2.5x10^5$ cells were

transfected with 55 pmol siRNA using 2 µl of JetPRIME Transfection reagent and 50 µl of JetPRIME buffer. Then, 48 h after transfection, cells were analyzed by semi-quantitative PCR or western-blot (WB).

RNA Extraction, cDNA Synthesis, Semi-Quantitative PCR and Real Time Quantitative PCR (qPCR)

RNA was extracted from cell lines using TRIzol reagent (Sigma) and the RNeasy Mini Kit (Qiagen Inc.) according to manufacturer's instructions. The RNA was quantified using a NanoDrop ND-1000 spectrophotometer (NanoDrop Technologies Inc.) and used for cDNA synthesis using the NZY First-Strand cDNA Synthesis Kit (NZYtech). cDNA was used for semi-quantitative PCR using PTPRN specific primers to evaluate gene silencing (Supplementary Table 2). Alternatively, cDNA was used for semi-quantitative PCR (two replicates) and/or qPCR (two replicates in duplicate) analyses upon transient PTPRN depletion of i) dysregulation of epithelial-mesenchymal transition (EMT) markers using specific primers of TGFβ1, Snail1 (SNAI1 gene), Claudin-2, E-Cadherin (CDH1), N-Cadherin (CDH2), and ZO1 (TJP1 gene), and ii) the analysis of insulin receptor signaling pathway using specific primers of mTOR, FOXO1, AS160, ERK1, ERK2, IRS1, AKT1, AKT2, and GSK3α (Supplementary Table 2). 18S was used as internal loading control. Semi-quantitative PCR reactions were performed using the Phusion High-Fidelity DNA Polymerase (Thermo Fisher Scientific). For qPCR, reactions were performed using TB-Green Premix Ex Taq Taq (Tli RNaseH plus, Takara), and PCR and data collection were performed on a Light Cycler 480 (Roche). All quantitations were normalized using human 18S.

Invasion, Proliferation, and Wound Healing Assays

Invasion, proliferation and wound healing assays were performed in duplicate as previously done (37). See Supplementary Material for information in detail.

***In vivo* Animal Experiments**

The Ethical Committee of the Instituto de Salud Carlos III (Spain) approved the protocols used for experimental work with mouse after approval for the ethical committee OEBA (Proex 285/19). For liver homing analysis, Nude mice were intrasplenically inoculated with $1x10^6$ KM12SM cells after 24h of transiently transfection with PTPRN (n=1 per siRNA) or control (n=2) siRNAs in 0.1 ml PBS. Mice were euthanized 24 h after intrasplenical cell inoculation, and RNA from liver and spleen isolated using TriZol Reagent. RNA was analyzed by RT-PCR to amplify human GAPDH and murine β-actin as loading control using specific primers (Supplementary Table 2). For metastasis experiments, $1x10^6$ KM12SM-vLuc liver metastatic CRC cells after 24h of transiently transfection with PTPRN or control siRNAs were intrasplenically injected in Nude mice (Charles River) in 0.1 ml PBS. The spleen was resected the day after, and then mice were daily inspected. Two weeks after intrasplenical cell inoculation, liver metastases were quantified in isoflurane anesthetized mice by luminescent activity of KM12SM-vLuc cells using luciferin (12.5 mg/kg; intraperitoneal injection). Luminescence was recorded with the IVIS *in vivo* imaging system (Perkin Elmer) every 7 days up to 60 days after intrasplenical cell injection. At day 60, mice were sacrificed, and inspected visually and by luminescence for the presence of liver metastasis.

Statistical Analysis

Data are presented as mean ± standard deviation (SD). All statistical analyses were performed with Microsoft Office Excel and the R program (version 3.6.1). For the analysis of the seroreactivity assays, the evaluation of the statistical significance between groups was performed using the t-test, and p values < 0.05 were considered statistically significant. Parametric test (t-test) was used having into account that our sample size was large enough (>30), without outliers, and with the mean of the data of the groups mostly representing the center of the distribution of the data. The diagnostic ability of PTPRN and ECD and ICD domains was evaluated by receiver operating characteristic (ROC) curves. ROC curves, their corresponding area under the curve (AUC) and maximized sensitivity and specificity values were calculated using the R package Epi (38).

For the analysis of the *in vitro* assays and qPCR data, the evaluation of the statistical significance between groups was performed using the t-test, and p values < 0.05 were considered statistically significant.

Data and Resource Availability

All data generated or analyzed during this study are included in this published article or available upon request.

RESULTS

Since T2D patients are at higher risk than non-diabetic patients to develop CRC (2; 24), we hypothesized that PTPRN could be dysregulated in CRC, and molecularly associated to the co-occurrence of cancer in type 2 diabetic patients.

Meta-Analysis of PTPRN in CRC

First, the potential alteration of PTPRN in colorectal cancer was evaluated by meta-analysis using public databases. The exam of the Oncomine database revealed higher mRNA expression of PTPRN in CRC compared to normal tissue (Fig. 1*A*) (39; 40). The exam of the TCGA cohort related to colon adenocarcinoma (COAD) and rectal adenocarcinoma (READ) revealed PTPRN mutations in almost 3% of CRC patients (Fig. 1*B*). Seven mutations leading to the loss of phosphatase function were found. Lastly, the COAD and READ TCGA datasets were used for PTPRN associated survival analysis assessed by Kaplan-Meier curves using the median for separating high and low PTPRN expression. The significance of the difference in survival between both populations was estimated by the log-rank test. An inverse association between PTPRN expression and overall or disease-free survival of colon adenocarcinoma and colorectal cancer was revealed (p values < 0.05) (Fig. 1*C*). For overall survival analysis, only 40% of CRC patients with high PTPRN expression levels survived about 6 years. In contrast, 75% of CRC patients with low PTPRN expression levels survived 6 years or longer. Moreover, for disease-free survival analysis, 40% of CRC patients with high PTPRN expression levels showed no recurrence after 6 years of diagnosis in comparison to the 65% of CRC patients showing low PTPRN expression levels.

Collectively, these data show that PTPRN alterations are present in CRC, with high PTPRN expression associated with a worse prognosis, indicating that PTPRN expression levels could be used as a malignant prognostic factor in the disease.

In Vitro Expression of PTPRN and Evaluation of its Humoral Immune Response

Then, since protein alterations have been associated to the development of humoral immune responses in cancer patients (41; 42), the ability of PTPRN to induce a humoral immune response in CRC patients was evaluated. Given that PTPRN is recognized by autoantibodies of T1D patients, we also evaluated if the population with T2D, which has an increased CRC risk, presents PTPRN autoantibodies.

To this end, we produced the protein *in vitro* and measured the specific immunoreactivity present in the plasma of patients with T2D or CRC or both, compared to healthy subjects. Full-length PTPRN, as well as its ICD and ECD domains (Fig. 2*A*), were expressed fused to HaloTag in the C-terminal end using an *in vitro* cell-free expression system (33; 34; 36). HaloTag allows purifying the fusion proteins by covalent immobilization with magnetic beads (MBs) for direct evaluation of autoantibody levels in plasma samples.

Fusion proteins were correctly expressed (Fig. 2*B*) and immobilized onto the MBs (Fig. 2*C*) with no degradation that could interfere in the screening as shown by immunostaining. HaloTag functionality was verified by incubation of the fusion proteins with chloroalkane functionalized MBs that covalently bound HaloTag and an antibody specific against the tag. Signal was developed in all cases, indicating that the tag (fused to the proteins) was successfully attached into the MBs surface (Fig. 2*C*).

Once established the optimal working conditions, we evaluated whether PTPRN or its domains could discriminate between CRC, T2D, or T2D with CRC patients, or healthy individuals (Fig. 2*D*). To this end, plasma samples were separately evaluated for the control groups (healthy and T2D individuals) *versus* the CRC group (with or without T2D). When the seroreactivity of samples from T2D patients with or without CRC was evaluated against the fusion proteins, both PTPRN full-length and ECD were able to discriminate colorectal cancer patients from controls ($p < 0.03$) (Fig. 2*E*), whereas ICD showed no discrimination potential and similar high background or unspecific signal in both groups. PTPRN and ECD seroreactivity were higher in patients with CRC or with T2D and CRC as compared to the control group (Fig. 2*F*). However, only full-length PTPRN could significantly discriminate between controls and T2D patients with CRC. On the other hand, only ECD could discriminate with statistical

significance between the control group and CRC patients (Fig. 2*F*). The data suggest that the seroreactivity present in patients with CRC is mainly directed towards ECD. As control of the specificity of the assay, seroreactivity towards Epstein Barr Antigen 1 (EBNA1) was evaluated in parallel. No significant differences (p values >0.1) were found among all groups (Fig. 2*G*).

Finally, comparison of the seroreactivity of T2D patients with and without CRC revealed that full-length PTPRN discriminated with statistical significance the presence/absence of CRC in T2D patients (Fig. 2*H*). Therefore, PTPRN appeared as a useful blood-based biomarker to discriminate CRC in T2D patients.

Diagnostic Ability of PTPRN in Patients with CRC

Lastly, to evaluate the diagnostic potential of the detection of autoantibodies, we obtained ROC curves. When discriminating control and CRC groups using autoantibodies against PTPRN (full-length and ECD), an overall AUC of 76.5% (sensitivity 55.6%, specificity 95.0%) was found, suggesting their potential for the detection of the pathology (Fig. 3*A*). Furthermore, an overall AUC of 90.0% (sensitivity 75.0%, specificity 100%) was found to discriminate T2D patients with CRC from those without. The results indicate the usefulness of PTPRN full-length and ECD autoantibodies to screen T2D patients with a potential risk of developing CRC (Fig. 3*B*).

PTPRN Depletion Reduces the Tumorigenic Properties of Colorectal Cancer Cell Lines

To understand how PTPRN influences the tumorigenic properties of CRC, we used two isogenic CRC cell lines with opposite metastatic properties. Liver metastatic KM12SM cells show the highest levels of PTPRN expression (Fig. 4*A*), in contrast to non-metastatic KM12C cells.

PTPRN transient silencing followed by invasion, proliferation and wound healing assays was used in KM12C and KM12SM cells compared to scrambled cells to assess PTPRN influence in tumorigenic and metastatic properties. First, depletion of PTPRN by transient silencing using

three different siRNAs was efficiently achieved as observed by PCR and WB analyses (Fig. 4*B*). Next, tumorigenic and metastatic properties were assessed.

Using Matrigel invasion assays, PTPRN-depleted KM12C and KM12SM CRC cell lines exhibited reduced invasiveness as compared with scrambled control cells using the three independent PTPRN siRNAs (p values < 0.05) (Fig. 4*C*). Next, in proliferation assays PTPRN-depleted KM12C and KM12SM cells proliferated less with PTPRN siRNAs #1 and #3 than control cells transfected with the scrambled siRNA (p values < 0.05, Fig. 4*D*). Consistent with their origin and different metastatic properties, there were more KM12SM cells capable of invading the Transwell chamber through the Matrigel than KM12C cells. In addition, KM12SM cells showed higher proliferation rates than non-metastatic primary tumor KM12C cells.

Since invasion appeared to be more affected than proliferation by PTPRN silencing, wound healing assays were used to confirm a role of PTPRN on cell migration using PTPRN siRNA #1 (Fig. 4*E*). KM12SM cells tend to close the wound faster than KM12C. Both PTPRN-silenced cell lines closed the wound at a slower rate than their control cells transfected with the scramble siRNA with a significantly higher effect on KM12SM cells (Fig. 4*E*), whose PTPRN expression was higher (Fig. 4*A*). The speed of migration was calculated for both conditions. The primary control cells KM12C cells transfected with scrambled siRNA migrated at an average speed of 102 ± 5 pixels/h, while KM12C cells transfected with PTPRN siRNA migrated at an average speed of 71 ± 28 pixels/h indicating a 30% reduction in the migration speed after PTPRN depletion. Likewise, the average migration speed was decreased in the metastatic KM12SM cells upon PTPRN depletion. Consistent with their origin, the average migration speed of the metastatic KM12SM cells was higher than that of KM12C cells, and it decreased from values of 140 ± 82 pixels/h, to 109 ± 34 pixels/h for the cells transiently transfected with scrambled and PTPRN siRNAs, respectively.

PTPRN Silencing on Metastatic Colorectal Cancer Cell Lines Reduces the Expression of Inducers of the Mesenchymal Phenotype

Epithelial-mesenchymal transition (EMT) of epithelial cells is associated to malignancy and supports changes in cell proliferation, migration and invasion, which were reduced by PTPRN depletion in our assays. Therefore, we investigated whether PTPRN depletion alters EMT inducers in CRC cells (Fig. 5*A,B*).

Changes in the mRNA expression levels of TGFβ1, Snail1 (SNAI1 gene), Claudin-2, E-Cadherin (CDH1), N-Cadherin (CDH2), and ZO1 (TJP1 gene) were analyzed by semi-quantitative PCR (Fig. 5*A*) and qPCR (Fig. 5*B*) analyses. PTPRN depletion caused in both KM12C and KM12SM cells a significantly decrease in EMT inducers TGFβ1, and SNAI1. Moreover, a slight dysregulation of tight junctions' proteins ZO1 and Claudin-2 suggested that PTPRN depletion provokes at least a partial reversion of the EMT transition. Differences were more pronounced in KM12SM highly metastatic colorectal cancer cells to liver than in KM12C cells; where the decrease in the EMT inducers SNAI1 and TGFβ1 was surprisingly not accompanied by an increase in the epithelial marker E-Cadherin and a decrease of N-Cadherin. Although quantitative results corroborated the dysregulation of EMT markers observed by semi-quantitative PCR analyses, further studies are needed to understand whether these proteins are further regulated post-transcriptionally.

PTPRN Depletion Alters the Insulin Receptor Signaling Pathway

We next explored whether PTPRN depletion in isogenic non-metastatic and metastatic CRC cells could also affect insulin receptor signaling, as a surrogate marker of the interrelationship of PTPRN between T2D and cancer. To this end, the expression levels of insulin receptor and insulin receptor signaling intermediates were explored either by PCR, qPCR and/or WB (Fig. 5 *C,D*).

A decrease in the mRNA expression levels of IRS1, GSK3α, FOXO1, mTOR, AS160, AKT1, AKT2, ERK1 and ERK2 was observed upon PTPRN depletion in both KM12C and KM12SM cells by semi-quantitative PCR and/or qPCR analyses (Fig. 5*C,D*), showing that PTPRN depletion impact insulin receptor signaling by altering the basal levels of its intermediate molecules. Again, quantitative results, which showed a similar alteration in IR

signaling with the three siRNAs, corroborated observations at semi-quantitative level. WB for IRS1, AKT, and ERK confirmed previous results on mRNA (Fig. 5*E*). In addition, as observed by WB, PTPRN depletion decreased precursor and mature pIRβ, pAKT, pERK and pFOXO1/3 protein levels in KM12C and KM12SM cells. On the contrary, GSK3β at protein level was overexpressed upon PTPRN depletion.

Collectively, albeit certain variability attributable to the use of three independent siRNAs, data suggests that PTPRN depletion alters insulin receptor signaling. This alteration in turn contributes to the dysregulation of the EMT, leading to a partial reduction of the EMT process with the subsequent diminished proliferation, migration and invasion observed in CRC cells.

PTPRN Depletion Decreases Liver Metastasis Ability of CRC Cells

In vivo effects of the transiently PTPRN depletion was investigated on KM12SM CRC liver metastatic cells. First, KM12SM cells were inoculated in the spleen of nude mice to examine PTPRN effects on the capacity for liver homing. As a surrogate marker for homing, human GAPDH was barely detected in the livers of mice inoculated with transiently transfected siRNAs #1 and #2 against PTPRN or decreased (#3) in comparison to KM12SM cells transfected with scramble (Fig. 6*A*).

Therefore, as PTPRN seems to be important for liver homing and metastatic colonization in CRC, we further studied the role of PTPRN on metastasis formation and growth. After intrasplenic inoculation of KM12SM-vLuc cells transiently transfected with siRNAs 24h prior to inoculation, luciferase expression was assessed as a proxy of liver metastatic growth every 7 days from day 20 to day 60, where control mice started showing distress signs (Fig. 6*B*). Interestingly, PTPRN depleted cells upon intrasplenical injection developed significantly lower or non-detectable liver metastatic foci in comparison to control cells (Fig. 6*B,C*). Finally, livers from all animals were further visualized by luminescence (Fig. 6*D*). Liver metastatic foci were present in the two control mice. In contrast, only 1 out of 6 mice inoculated with PTPRN depleted cells developed substantially smaller metastatic foci. Reduced metastatic formation and

growth was associated with the lower capacity for liver colonization of PTPRN depleted cells. These results suggest that PTPRN is required in CRC cells for liver metastasis *in vivo*.

DISCUSSION

Dysregulated signaling pathways and specifically signaling by protein tyrosine-kinases is a hallmark of many cancers and of metabolic diseases such as diabetes, which have been extensively studied. In contrast, the role of tyrosine-phosphatases (including PTPRN), which may play an important role in the tumorigenic process as signaling inactivators, remains unclear (43) although some tyrosine phosphatases receptors alterations were observed in cancer (7). Tyrosine phosphatases dephosphorylate tyrosine residues, and have a potential to regulate physiological processes relevant in cancer development as cell proliferation, differentiation, adhesion, and migration. Therefore, cellular homeostasis requires tight regulation of tyrosine phosphatases, and their dysregulation may contribute to the development of diseases. As such, numerous genetic and epigenetic alterations have been described for PTPR receptors including amplification, deletion, and mutations in PTPRN (43).

Increasing evidences reveal a relationship between diabetes and many cancers (2). Several epidemiologic studies have found that diabetic patients are at increased risk of developing CRC compared to non-diabetic individuals (2; 44; 45). This relationship is especially relevant in T2D patients, a disease that develops slowly with early symptoms being frequently silent until diagnosis. Since PTPRN is a well-established diabetes autoantibody, albeit for type 1 diabetic patients, and since autoantibodies have been shown to be useful for cancer diagnosis (41), we studied here whether the presence of PTPRN autoantibodies might represent another link between diabetes and CRC.

Therefore, we have evaluated the potential implication of PTPRN in CRC and T2D. Overall, a direct association between seroreactivity towards PTPRN in CRC patients and malignancy was observed. Surprisingly, PTPRN autoantibody levels in plasma were a good discriminator between patients with and without CRC for non-diabetic patients and even better for T2D patients. Moreover, since ICD seroreactivity was observed at a similar extent for controls and CRC patients, ECD seemed to be the domain of the protein that induced such response. In addition, CRC patients with and without type 2 diabetes showed increased levels of autoantibodies against PTPRN and ECD when compared individually to the control group. ROC

curves with the data gathered for the control subjects and CRC group showed an overall AUC of 76.5%, indicating the usefulness of PTPRN as CRC diagnostic autoantibody marker. When comparing the diagnostic potential of autoantibodies to PTPRN and ECD in T2D patients with and without CRC, an AUC of 90% was achieved. Remarkably, the data suggest that PTPRN and ECD autoantibodies could be used to evaluate the risk of CRC in T2D patients. To our knowledge, this is the first study linking diabetes and cancer by means of seroreactive analysis of autoantibodies. Given the increased risk of CRC for T2D patients, our results may translate into preventive strategies on the management of T2D patients.

Through functional *in vitro* cell-based assays and *in vivo* assays, it was made evident that PTPRN silencing produced a shift on the tumorigenic and metastatic properties of the studied colon cancer cell lines. KM12C and KM12SM cell lines lost invasion, proliferation, and migration abilities upon PTPRN depletion. *In vivo*, PTPRN depletion led to a loss in liver homing and metastatic ability of KM12SM cells. These results suggest that PTPRN plays a role along the progression of CRC, in both primary tumor (KM12C cells) and in metastasis (KM12SM cells). In this sense, and considering the relationship between tumorigenic properties of cancer cells and EMT, the expression of EMT effectors after PTPRN transient depletion reflected a dysregulation on the expression of Snail1, TGFβ1, E-Cadherin and N-Cadherin, among other EMT effectors and transcription factors (TF) that may account for the observed partial reversion of the epithelial-mesenchymal transition. Surprisingly the downregulation of TGFβ1 and Snail1was not accompanied by the opposite up-regulation and down-regulation of of E-Cadherin and N-Cadherin, respectively. This could be associated to the powerful features of EMT-TFs and their relevance for cancer pathogenesis (46-48), from tumor initiation, establishment of precursor lesions, accumulation of genetic alterations, escape from tumor surveillance, therapy resistance to the development of metastasis (48; 49). These processes provoke a continuous flux between epithelial and mesenchymal end point states (47; 48), which is often partially executed (46). Indeed, it has been described a rebound effect in some EMT effectors (i.e. Slug and Snail (50)) (46), which could be associated to this unexpected feature, and to a partial EMT dysregulation. Further studies using stably transfected cell lines are needed

to elucidate the interactor proteins of PTPRN and its effectors, and to understand in detail how PTPRN contributes to the EMT process. However, present data suggests that PTPRN may represent an interesting therapeutic target for CRC and for metastatic CRC to liver. Finally, it is also noteworthy that PTPRN depletion causes also a decrease in the insulin receptor signaling, and in ERK and AKT that might also explain the changes observed in the expression of EMT genes, and the decrease in proliferation, migration and invasion of CRC cells *in vitro,* respectively. Noticeably, the decrease on ERK and AKT mRNA and protein levels could be associated to i) the dysregulation of the insulin receptor signaling, ii) a decrease in PTPRN signaling -whose depletion decreased proliferation, invasion and migration of CRC cells, processes where AKT and ERK are implicated (43)-, or iii) synergistic effects on the dysregulation of both signaling routes. These results further support a role for PTPRN as a link between cancer and diabetes.

Notably, although higher patient samples and multicentric cohorts together with other added factors such as hyperinsulinemia should be analyzed in subsequent studies to get further evidences of the role of PTPRN in cancer and diabetes and to overcome some limitations in the study as the number of samples, we have demonstrated here a significant relationship between PTPRN, T2D and colorectal cancer progression. These results demonstrate a new link between these highly prevalent chronic diseases. Moreover, *in vitro* and *in vivo* assays using stably-transfected CRC cells will help to evaluate the mechanisms of action of PTPRN on EMT transition, and on ERK and AKT and insulin receptor signaling pathways. Future studies on PTPRN dysregulation in CRC patients with and without T2D are guaranteed to shed light on its potential for screening T2D diabetes patients for CRC. Additionally, PTPRN may offer a new potential therapeutic target in CRC in a clinical setting.

Supplementary Information. This article contains supplementary material online.

Acknowledgements. We thank the excellent technical support of MariCruz Sánchez-Martínez.

Funding. This work was supported by the Ramon y Cajal programme of the MINECO and the financial support of the PI17CIII/00045 and PI20CIII/00019 grants partially supported by FEDER funds from the AES-ISCIII program to R.B., and Mineco/FEDER SAF2016-79837-R and PID2019-110998RB-I00 to C.G-J. M.G-A. was supported by a contract of the Programa Operativo de Empleo Juvenil y la Iniciativa de Empleo Juvenil (YEI) with the participation of the Consejería de Educación, Juventud y Deporte de la Comunidad de Madrid y del Fondo Social Europeo. The FPU predoctoral contract to A.M-C. is supported by the Spanish Ministerio de Educación, Cultura y Deporte. G.S-F. is recipient of a predoctoral contract (grant number 1193818N) supported by The Flanders Research Foundation (FWO).

Duality of interest. The authors declare no conflict of interest.

Author contributions. All authors meet the requirements for authorship. M.G-A., G.S-F., A.M-C., JM.G-M., C.F., P.P., N. P-G., and A.G-A. performed the experiments. C.G-J., A.G-A. and R.B. designed the experiments. M.G-A., G.S-F., A.M-C., C.G-J., A.G-A. and R.B. analyzed the data and wrote the manuscript. M.G-A. and R.B. are the guarantors of this work and, as such, had full access to all of the data in the study, and take responsibility for the integrity of the data and the accuracy of the data analysis.

References

1. American Diabetes A: Diagnosis and classification of diabetes mellitus. Diabetes Care 2013;36 Suppl 1:S67-74
2. Garcia-Jimenez C, Gutierrez-Salmeron M, Chocarro-Calvo A, Garcia-Martinez JM, Castano A, De la Vieja A: From obesity to diabetes and cancer: epidemiological links and role of therapies. Br J Cancer 2016;114:716-722
3. Alonso A, Sasin J, Bottini N, Friedberg I, Friedberg I, Osterman A, Godzik A, Hunter T, Dixon J, Mustelin T: Protein tyrosine phosphatases in the human genome. Cell 2004;117:699-711
4. Johnson KG, Van Vactor D: Receptor protein tyrosine phosphatases in nervous system development. Physiol Rev 2003;83:1-24
5. Hendriks WJ, Elson A, Harroch S, Stoker AW: Protein tyrosine phosphatases: functional inferences from mouse models and human diseases. FEBS J 2008;275:816-830
6. Stoker A: Methods for identifying extracellular ligands of RPTPs. Methods 2005;35:80-89
7. Julien SG, Dube N, Hardy S, Tremblay ML: Inside the human cancer tyrosine phosphatome. Nat Rev Cancer 2011;11:35-49
8. Harashima S, Horiuchi T, Wang Y, Notkins AL, Seino Y, Inagaki N: Sorting nexin 19 regulates the number of dense core vesicles in pancreatic beta-cells. J Diabetes Investig 2012;3:52-61
9. Lampasona V, Bearzatto M, Genovese S, Bosi E, Ferrari M, Bonifacio E: Autoantibodies in insulin-dependent diabetes recognize distinct cytoplasmic domains of the protein tyrosine phosphatase-like IA-2 autoantigen. J Immunol 1996;157:2707-2711
10. Xie H, Notkins AL, Lan MS: IA-2, a transmembrane protein tyrosine phosphatase, is expressed in human lung cancer cell lines with neuroendocrine phenotype. Cancer Res 1996;56:2742-2744
11. Notkins AL, Lan MS, Leslie RD: IA-2 and IA-2beta: the immune response in IDDM. Diabetes Metab Rev 1998;14:85-93
12. Zhangyuan G, Yin Y, Zhang W, Yu W, Jin K, Wang F, Huang R, Shen H, Wang X, Sun B: Prognostic Value of Phosphotyrosine Phosphatases in Hepatocellular Carcinoma. Cell Physiol Biochem 2018;46:2335-2346
13. Yin W, Tang G, Zhou Q, Cao Y, Li H, Fu X, Wu Z, Jiang X: Expression Profile Analysis Identifies a Novel Five-Gene Signature to Improve Prognosis Prediction of Glioblastoma. Front Genet 2019;10:419
14. Xu H, Cai T, Carmona GN, Abuhatzira L, Notkins AL: Small cell lung cancer growth is inhibited by miR-342 through its effect of the target gene IA-2. J Transl Med 2016;14:278
15. Shergalis A, Bankhead A, 3rd, Luesakul U, Muangsin N, Neamati N: Current Challenges and Opportunities in Treating Glioblastoma. Pharmacol Rev 2018;70:412-445
16. Bauerschlag DO, Ammerpohl O, Brautigam K, Schem C, Lin Q, Weigel MT, Hilpert F, Arnold N, Maass N, Meinhold-Heerlein I, Wagner W: Progression-free survival in ovarian cancer is reflected in epigenetic DNA methylation profiles. Oncology 2011;80:12-20
17. Nesterova M, Johnson N, Cheadle C, Cho-Chung YS: Autoantibody biomarker opens a new gateway for cancer diagnosis. Biochim Biophys Acta 2006;1762:398-403
18. Noaki R, Kawahara H, Watanabe K, Ushigome T, Kobayashi S, Yanaga K: Serum p53 antibody is a useful tumor marker of early colorectal cancer. International surgery 2010;95:287-292
19. Barderas R, Villar-Vazquez R, Fernandez-Acenero MJ, Babel I, Pelaez-Garcia A, Torres S, Casal JI: Sporadic colon cancer murine models demonstrate the value of autoantibody detection for preclinical cancer diagnosis. Scientific reports 2013;3:2938
20. Pedersen JW, Gentry-Maharaj A, Fourkala EO, Dawnay A, Burnell M, Zaikin A, Pedersen AE, Jacobs I, Menon U, Wandall HH: Early detection of cancer in the general population: a blinded case-control study of p53 autoantibodies in colorectal cancer. Br J Cancer 2013;108:107-114
21. Qiu J, Choi G, Li L, Wang H, Pitteri SJ, Pereira-Faca SR, Krasnoselsky AL, Randolph TW, Omenn GS, Edelstein C, Barnett MJ, Thornquist MD, Goodman GE, Brenner DE, Feng Z,

Hanash SM: Occurrence of autoantibodies to annexin I, 14-3-3 theta and LAMR1 in prediagnostic lung cancer sera. J Clin Oncol 2008;26:5060-5066
22. Dudas SP, Chatterjee M, Tainsky MA: Usage of cancer associated autoantibodies in the detection of disease. Cancer Biomark 2010;6:257-270
23. Yao C, Nash GF, Hickish T: Management of colorectal cancer and diabetes. J R Soc Med 2014;107:103-109
24. Gutierrez-Salmeron M, Chocarro-Calvo A, Garcia-Martinez JM, de la Vieja A, Garcia-Jimenez C: Epidemiological bases and molecular mechanisms linking obesity, diabetes, and cancer. Endocrinol Diabetes Nutr 2017;64:109-117
25. Gutierrez-Salmeron M, Lucena SR, Chocarro-Calvo A, Garcia-Martinez JM, Martin Orozco RM, Garcia-Jimenez C: Metabolic and hormonal remodeling of colorectal cancer cell signalling by diabetes. Endocr Relat Cancer 2021;28:R191-R206
26. Babel I, Barderas R, Diaz-Uriarte R, Martinez-Torrecuadrada JL, Sanchez-Carbayo M, Casal JI: Identification of tumor-associated autoantigens for the diagnosis of colorectal cancer in serum using high density protein microarrays. Mol Cell Proteomics 2009;8:2382-2395
27. Babel I, Barderas R, Diaz-Uriarte R, Moreno V, Suarez A, Fernandez-Acenero MJ, Salazar R, Capella G, Casal JI: Identification of MST1/STK4 and SULF1 proteins as autoantibody targets for the diagnosis of colorectal cancer by using phage microarrays. Mol Cell Proteomics 2011;10:M110 001784
28. Barderas R, Babel I, Diaz-Uriarte R, Moreno V, Suarez A, Bonilla F, Villar-Vazquez R, Capella G, Casal JI: An optimized predictor panel for colorectal cancer diagnosis based on the combination of tumor-associated antigens obtained from protein and phage microarrays. Journal of proteomics 2012;75:4647-4655
29. Morikawa K, Walker SM, Nakajima M, Pathak S, Jessup JM, Fidler IJ: Influence of organ environment on the growth, selection, and metastasis of human colon carcinoma cells in nude mice. Cancer Res 1988;48:6863-6871
30. Morikawa K, Walker SM, Jessup JM, Fidler IJ: In vivo selection of highly metastatic cells from surgical specimens of different primary human colon carcinomas implanted into nude mice. Cancer Res 1988;48:1943-1948
31. Brennan TV, Lin L, Huang X, Yang Y: Generation of Luciferase-expressing Tumor Cell Lines. Bio Protoc 2018;8
32. Garranzo-Asensio M, Guzman-Aranguez A, Povedano E, Ruiz-Valdepenas Montiel V, Poves C, Fernandez-Acenero MJ, Montero-Calle A, Solis-Fernandez G, Fernandez-Diez S, Camps J, Arenas M, Rodriguez-Tomas E, Joven J, Sanchez-Martinez M, Rodriguez N, Dominguez G, Yanez-Sedeno P, Pingarron JM, Campuzano S, Barderas R: Multiplexed monitoring of a novel autoantibody diagnostic signature of colorectal cancer using HaloTag technology-based electrochemical immunosensing platform. Theranostics 2020;10:3022-3034
33. Garranzo-Asensio M, Guzman-Aranguez A, Poves C, Fernandez-Acenero MJ, Torrente-Rodriguez RM, Ruiz-Valdepenas Montiel V, Dominguez G, Frutos LS, Rodriguez N, Villalba M, Pingarron JM, Campuzano S, Barderas R: Toward Liquid Biopsy: Determination of the Humoral Immune Response in Cancer Patients Using HaloTag Fusion Protein-Modified Electrochemical Bioplatforms. Anal Chem 2016;88:12339-12345
34. Garranzo-Asensio M, San Segundo-Acosta P, Poves C, Fernandez-Acenero MJ, Martinez-Useros J, Montero-Calle A, Solis-Fernandez G, Sanchez-Martinez M, Rodriguez N, Ceron MA, Fernandez-Diez S, Dominguez G, de Los Rios V, Pelaez-Garcia A, Guzman-Aranguez A, Barderas R: Identification of tumor-associated antigens with diagnostic ability of colorectal cancer by in-depth immunomic and seroproteomic analysis. Journal of proteomics 2020;214:103635
35. Barderas R, Shochat S, Timmerman P, Hollestelle MJ, Martinez-Torrecuadrada JL, Hoppener JW, Altschuh D, Meloen R, Casal JI: Designing antibodies for the inhibition of gastrin activity in tumoral cell lines. Int J Cancer 2008;122:2351-2359
36. Garranzo-Asensio M, Guzman-Aranguez A, Poves C, Fernandez-Acenero MJ, Montero-Calle A, Ceron MA, Fernandez-Diez S, Rodriguez N, Gomez de Cedron M, Ramirez de Molina A, Dominguez G, Barderas R: The specific seroreactivity to Np73 isoforms shows higher

diagnostic ability in colorectal cancer patients than the canonical p73 protein. Scientific reports 2019;9:13547
37. Pelaez-Garcia A, Barderas R, Torres S, Hernandez-Varas P, Teixido J, Bonilla F, de Herreros AG, Casal JI: FGFR4 role in epithelial-mesenchymal transition and its therapeutic value in colorectal cancer. PLoS One 2013;8:e63695
38. Team RC: R: A language and environment for statistical computing. R Foundation for Statistical Computing, Vienna, Austria 2015;
39. Notterman DA, Alon U, Sierk AJ, Levine AJ: Transcriptional gene expression profiles of colorectal adenoma, adenocarcinoma, and normal tissue examined by oligonucleotide arrays. Cancer Res 2001;61:3124-3130
40. Kurashina K, Yamashita Y, Ueno T, Koinuma K, Ohashi J, Horie H, Miyakura Y, Hamada T, Haruta H, Hatanaka H, Soda M, Choi YL, Takada S, Yasuda Y, Nagai H, Mano H: Chromosome copy number analysis in screening for prognosis-related genomic regions in colorectal carcinoma. Cancer Sci 2008;99:1835-1840
41. Anderson KS, LaBaer J: The sentinel within: exploiting the immune system for cancer biomarkers. J Proteome Res 2005;4:1123-1133
42. Casal JI, Barderas R: Identification of cancer autoantigens in serum: toward diagnostic/prognostic testing? Mol Diagn Ther 2010;14:149-154
43. Du Y, Grandis JR: Receptor-type protein tyrosine phosphatases in cancer. Chin J Cancer 2015;34:61-69
44. Suh S, Kim KW: Diabetes and cancer: is diabetes causally related to cancer? Diabetes Metab J 2011;35:193-198
45. Cannata D, Fierz Y, Vijayakumar A, LeRoith D: Type 2 diabetes and cancer: what is the connection? Mt Sinai J Med 2010;77:197-213
46. Stemmler MP, Eccles RL, Brabletz S, Brabletz T: Non-redundant functions of EMT transcription factors. Nat Cell Biol 2019;21:102-112
47. Nieto MA, Cano A: The epithelial-mesenchymal transition under control: global programs to regulate epithelial plasticity. Semin Cancer Biol 2012;22:361-368
48. Nieto MA, Huang RY, Jackson RA, Thiery JP: Emt: 2016. Cell 2016;166:21-45
49. Puisieux A, Brabletz T, Caramel J: Oncogenic roles of EMT-inducing transcription factors. Nat Cell Biol 2014;16:488-494
50. Ganesan R, Mallets E, Gomez-Cambronero J: The transcription factors Slug (SNAI2) and Snail (SNAI1) regulate phospholipase D (PLD) promoter in opposite ways towards cancer cell invasion. Mol Oncol 2016;10:663-676

Table 1. Plasma samples used for the seroreactivity analysis of PTPRN and its domains.

Group	Samples (male/female)	Age (years; median ± standard deviation)
Control	4/6	44 ± 11
Type 2 diabetes	7/3	65 ± 12
CRC	6/4	70 ± 12
CRC with type 2 diabetes	5/3	65 ± 8

Legend to the Figures

Figure 1-Assessment of PTPRN dysregulation in CRC. *A:* Evaluation of mRNA levels in CRC tissue compared to normal adjacent tissue using Oncomine. Higher PTPRN mRNA levels were found in CRC tissue in comparison to control tissue (39; 40). *B*: The cBioPortal database retrieved data about the presence of PTPRN mutations at a genetic level in almost 3% of CRC patients (The Cancer Genome Atlas -Colon Adenocarcinoma-). CNA, Copy Number Alteration. *C*: Survival analysis retrieved from the GEPIA2 web-based tool revealed that a higher PTPRN expression in CRC patients (READ and COAD) and colon adenocarcinoma (COAD) patients (TCGA datasets) was related with a large decrease in their overall and disease free survival (*p* values < 0.05).

Figure 2-*In vitro* PTPRN expression and seroreactivity analysis of PTPRN. *A*: PTPRN (979 amino acids in length) is composed of a signal peptide (SP), an extracellular domain (ECD), a transmembrane domain (TMB), and an intracellular domain (ICD). The amino acids composing each domain are highlighted. *B*: Immunostaining using a monoclonal antibody against the HaloTag of the indicated fusion proteins *in vitro* expressed. *C*: Covalent immobilization of the proteins into magnetic beads (MBs) by HaloTag was verified through luminescence using a monoclonal antibody against the tag. *D*: Seroreactivity analysis of autoantibodies against ECD, ICD, and PTPRN in plasma samples from healthy individuals, and diabetic, CRC, and CRC with type 2 diabetes patients. *E*: PTPRN and ECD seroreactivity was significantly higher in the CRC group than in the control group (*p* value < 0.05). *F*: When comparing the control group with the CRC patients and the CRC with type 2 diabetes patients separately, PTPRN could significantly discriminate between controls and type 2 diabetes with CRC patients (*p* value < 0.05), whereas ECD could significantly discriminate between the control group and the CRC patients (*p* value < 0.05). *G*: Not statistically significant differences were found when comparing EBNA1 seroreactivity among groups. EBNA1 seroreactivity was used as control because >90% of the human population has antibodies against EBNA1. *H*: Both PTPRN and

ECD autoantibodies could discriminate between diabetic individuals and CRC patients and CRC patients with type 2 diabetes separately (*p* values < 0.05). Measurements were performed in triplicate. Bar graphs represent the mean±SD. (*E,F,H*) * = p< 0.05

Figure 3-Diagnostic potential of the detection of PTPRN autoantibodies. The diagnostic potential for the detection of autoantibodies against PTPRN and ECD was evaluated using ROC curves. *A*: Autoantibody detection could discriminate between control and CRC group with an AUC of 75.5%. *B*: Autoantibody detection could discriminate between type 2 diabetes patients and CRC with type 2 diabetes patients with an AUC of 90.0%.

Figure 4-Silencing of PTPRN in KM12C and KM12SM colorectal cancer cells and effect on their tumorigenic properties. *A*: Protein expression levels in CRC cell lines KM12C and KM12SM. RhoGDi was used as loading control. *B*: Evaluation by PCR and WB of the transient silencing of PTPRN after 48h post-transfection using three different siRNAs in KM12C and KM12SM cell lines. As control, we transfected the cell lines with a scrambled siRNA. By PCR, 18S was used as internal control. By WB, RhoGDi was used as loading control. *C,D*: PTPRN plays a role in the tumorigenic properties of metastatic colorectal cancer cell lines. KM12C and KM12SM transiently transfected with PTPRN siRNAs #1, #2 and #3 showed lower invasion capacity than control (scrambled transfected) cell lines (*p* values < 0.05). *D*: Both KM12C and KM12SM cell lines transiently transfected with PTPRN siRNAs #1 and #3 proliferate at a lower rate than control cells (*p* values < 0.05). *E*: Wound healing assays carried out during 48 h demonstrated that both cell lines migrated at a slower speed when PTPRN was depleted with PTPRN siRNA #1. In agreement with their metastatic properties, KM12SM cells showed higher invasion, proliferation and migration speed than KM12C cells. All experiments were performed in duplicate. Experiments performed with PTPRN siRNAs #1 and siRNAs #2 and #3 were performed separately.

Figure 5-PTPRN depletion on KM12C and KM12SM colorectal cancer cells alters EMT transition and reduces insulin receptor signaling pathway. *A,B*: Alterations in EMT inducers after PTPRN-depletion in KM12C and KM12SM cell lines. cDNA synthesized from total RNA from transiently-depleted PTPRN and scrambled control cells was subjected to (*A*) semi-quantitative RT-PCR analysis using specific primers for the EMT inducers TGFβ1, SNAI1, Claudin-2, E-Cadherin, N-Cadherin, and ZO1 using 18S as control and for normalization or (*B*) qPCR analysis using specific primers for TGFβ1, SNAI1, Claudin-2, and E-Cadherin using 18S for normalization. *C,D,E*: Analysis of alterations in the insulin receptor signaling pathway by PCR and WB, respectively, after PTPRN-depletion in KM12C and KM12SM cell lines. *C,D:* cDNA synthesized from total RNA from transiently-depleted PTPRN and scrambled control cells after 48h post-transfection was subjected to (*C*) semi-quantitative RT-PCR analysis using specific primers for IRS1, ERK1, ERK2, AKT1, AKT2, mTOR, FOXO1, AS160, and GSK3α using 18S as control and for normalization or (*D*) qPCR analysis using specific primers for ERK1, ERK2, AKT1, AKT2, mTOR, FOXO1, and GSK3α using 18S for normalization.. *E:* Protein expression levels of p-FOXO1/3, GSK3β, p-IRβ, AKT, p-AKT, ERK, p-ERK, and IRS1 in CRC cell lines KM12C and KM12SM transiently transfected with indicated siRNAs for 48h confirmed RT-PCR and/or qPCR results. GAPDH and RhoGDi were used as controls. Red Ponceau staining of each line was used for normalization. *A,C,E:* Two replicate experiments (1 and 2) were analyzed. Representative images are shown. *B,D:* Data represent the mean±SD of two experiments. The abundance of each mRNA and protein was quantified by densitometry using Image J.

Figure 6-PTPRN depletion decreases liver homing and liver metastasis in KM12SM CRC cells. *A:* Nude mice intrasplenically inoculated with KM12SM cells transiently transfected with siScramble (n=2) and indicated PTPRN siRNAs (n=1 per PTPRN siRNA) were sacrificed 24 hours after inoculation for analysis of in vivo liver homing. RNA was isolated from the liver and spleen (as control) and directly subjected to RT-PCR to amplify human GAPDH (hGAPDH). Representative experiments out of 2 are shown. Murine β-actin (mβ-actin) was

amplified as control. *B:* Representative images of luminescence intensity of *in vivo* luciferase activity from mice injected with KM12SM cells transiently transfected with control and PTPRN siRNAs at days 45 and 60 post-intrasplenical inoculation. Mice injected with control cells did show detectable bioluminescence by IVIS analyses, in contrast to mice injected with PTPRN depleted cells (1 out of 6 mice showed detectable luminescence signal). Three mice per group were inoculated, but 1 mouse of each group died prior to metastasis development because of other causes (i.e. after spleen resection, or hemorrhage), and thus n=2 was the final mice number per group at day 60. *C:* Luminescence per indicated mice was represented at each time points. *D:* At day 60 post-intrasplenical cell inoculation, livers from all control or PTPRN siRNA treated mice were collected and luminescence measured in an IVIS in vivo imaging system. As depicted in the images, 1 out of 6 PTPRN siRNA treated mice showed detectable luminescence, in contrast to the highly measurable luminescence of the two control siRNA mice. Significant luminescence values were observed comparing control and PTPRN siRNA groups, whose luminescence signal was represented by bar graph.

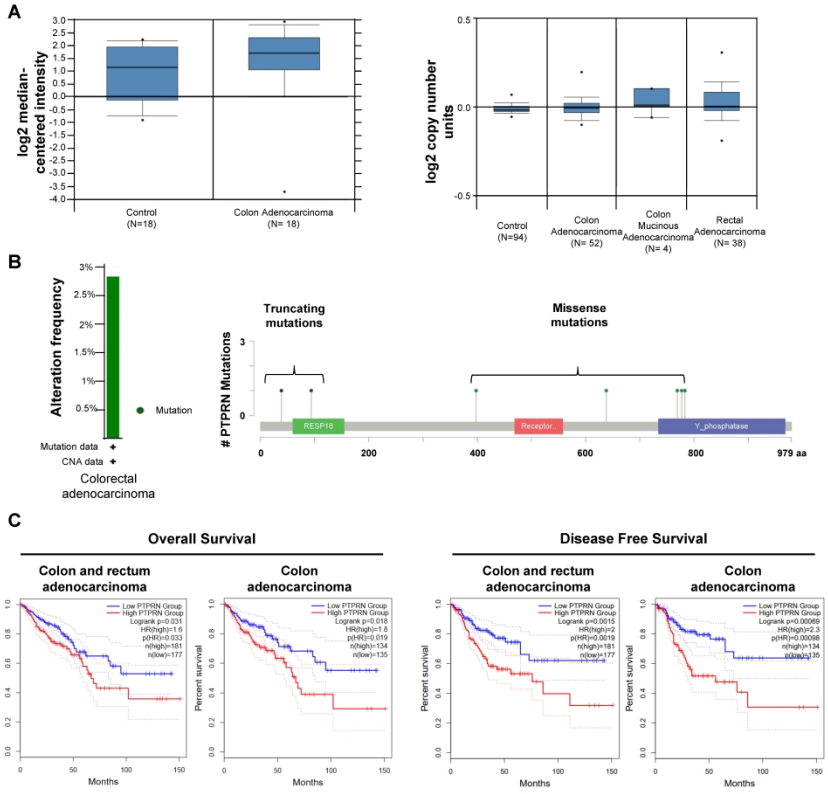

Figure 1

Figure 1-Assessment of PTPRN dysregulation in CRC. A: Evaluation of mRNA levels in CRC tissue compared to normal adjacent tissue using Oncomine. Higher PTPRN mRNA levels were found in CRC tissue in comparison to control tissue.(38; 39) B: The cBioPortal database retrieved data about the presence of PTPRN mutations at a genetic level in almost 3% of CRC patients (The Cancer Genome Atlas -Colon Adenocarcinoma-). CNA, Copy Number Alteration. C: Survival analysis retrieved from the GEPIA2 web-based tool revealed that a higher PTPRN expression in CRC patients (READ and COAD) and colon adenocarcinoma (COAD) patients (TCGA datasets) was related with a large decrease in their overall and disease free survival (p values < 0.05).

210x297mm (600 x 600 DPI)

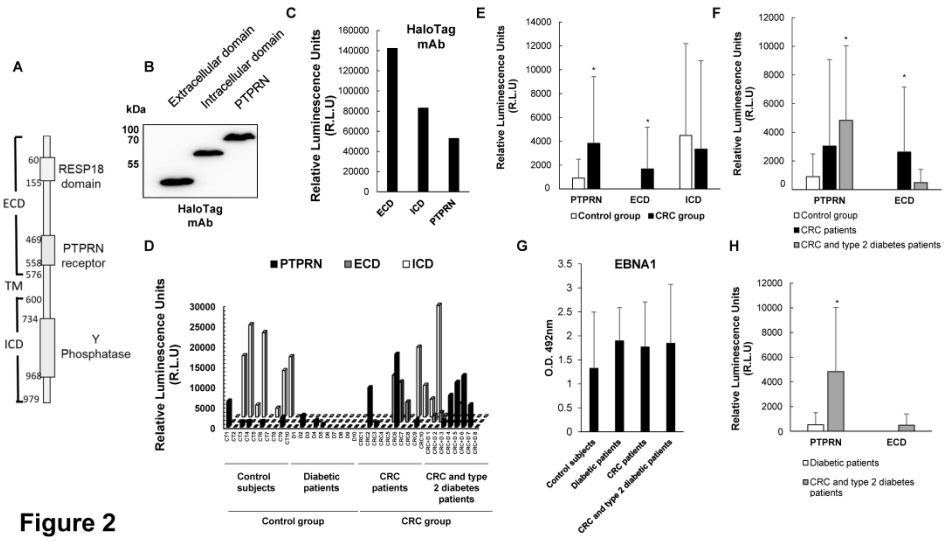

Figure 2

Figure 2-In vitro PTPRN expression and seroreactivity analysis of PTPRN. A: PTPRN (979 amino acids in length) is composed of a signal peptide (SP), an extracellular domain (ECD), a transmembrane domain (TMB), and an intracellular domain (ICD). The amino acids composing each domain are highlighted. B: Immunostaining using a monoclonal antibody against the HaloTag of the indicated fusion proteins in vitro expressed. C: Covalent immobilization of the proteins into magnetic beads (MBs) by HaloTag was verified through luminescence using a monoclonal antibody against the tag. D: Seroreactivity analysis of autoantibodies against ECD, ICD, and PTPRN in plasma samples from healthy individuals, and diabetic, CRC, and CRC with type 2 diabetes patients. E: PTPRN and ECD seroreactivity was significantly higher in the CRC group than in the control group (p value < 0.05). F: When comparing the control group with the CRC patients and the CRC with type 2 diabetes patients separately, PTPRN could significantly discriminate between controls and type 2 diabetes with CRC patients (p value < 0.05), whereas ECD could significantly discriminate between the control group and the CRC patients (p value < 0.05). G: Not statistically significant differences were found when comparing EBNA1 seroreactivity among groups. EBNA1 seroreactivity was used as control because >90% of the human population has antibodies against EBNA1. H: Both PTPRN and ECD autoantibodies could discriminate between diabetic individuals and CRC patients and CRC patients with type 2 diabetes separately (p values < 0.05). Measurements were performed in triplicate. Bar graphs represent the mean±SD. (E,F,H) * = p< 0.05

297x210mm (600 x 600 DPI)

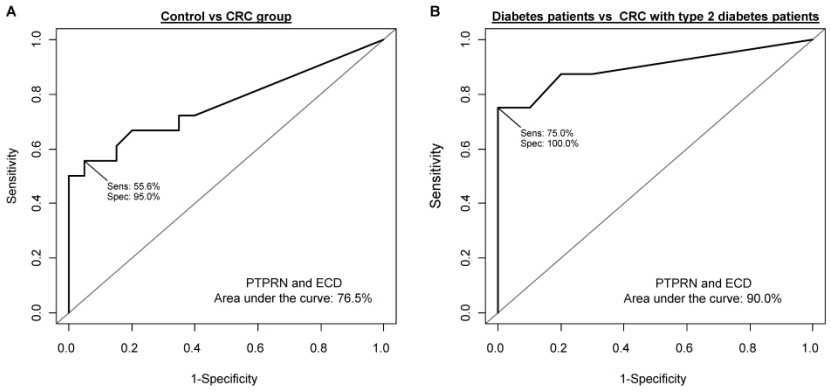

Figure 3

Figure 3-Diagnostic potential of the detection of PTPRN autoantibodies. The diagnostic potential for the detection of autoantibodies against PTPRN and ECD was evaluated using ROC curves. A: Autoantibody detection could discriminate between control and CRC group with an AUC of 75.5%. B: Autoantibody detection could discriminate between type 2 diabetes patients and CRC with type 2 diabetes patients with an AUC of 90.0%.

297x210mm (600 x 600 DPI)

Figure 4

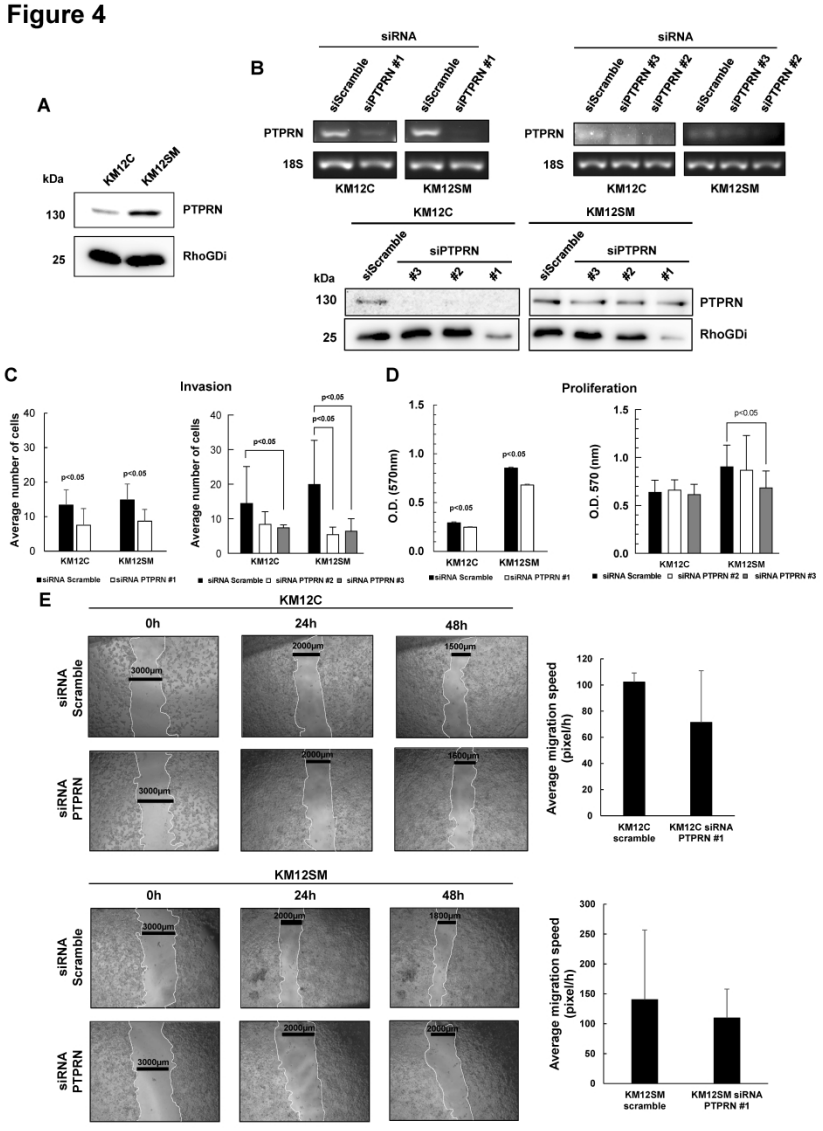

Figure 4-Silencing of PTPRN in KM12C and KM12SM colorectal cancer cells and effect on their tumorigenic properties. A: Protein expression levels in CRC cell lines KM12C and KM12SM. RhoGDi was used as loading control. B: Evaluation by PCR and WB of the transient silencing of PTPRN after 48h post-transfection using three different siRNAs in KM12C and KM12SM cell lines. As control, we transfected the cell lines with a scrambled siRNA. By PCR, 18S was used as internal control. By WB, RhoGDi was used as loading control. C,D: PTPRN plays a role in the tumorigenic properties of metastatic colorectal cancer cell lines. KM12C and KM12SM transiently transfected with PTPRN siRNAs #1, #2 and #3 showed lower invasion capacity than control (scrambled transfected) cell lines (p values < 0.05). D: Both KM12C and KM12SM cell lines transiently transfected with PTPRN siRNAs #1 and #3 proliferate at a lower rate than control cells (p values < 0.05). E: Wound healing assays carried out during 48 h demonstrated that both cell lines migrated at a slower speed when PTPRN was depleted with PTPRN siRNA #1. In agreement with their metastatic properties, KM12SM cells showed higher invasion, proliferation and migration speed than KM12C cells. All experiments were performed in duplicate. Experiments performed with PTPRN siRNAs #1 and siRNAs #2 and #3 were performed separately.

210x297mm (600 x 600 DPI)

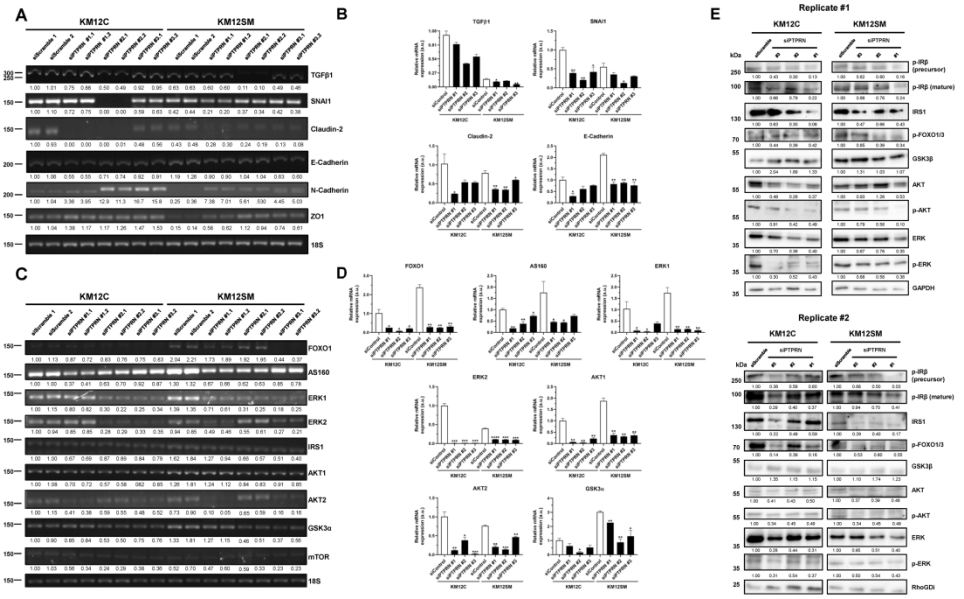

Figure 5

Figure 5-PTPRN depletion on KM12C and KM12SM colorectal cancer cells alters EMT transition and reduces insulin receptor signaling pathway. A,B: Alterations in EMT inducers after PTPRN-depletion in KM12C and KM12SM cell lines. cDNA synthesized from total RNA from transiently-depleted PTPRN and scrambled control cells was subjected to (A) semi-quantitative RT-PCR analysis using specific primers for the EMT inducers TGF□1, SNAI1, Claudin-2, E-Cadherin, N-Cadherin, and ZO1 using 18S as control and for normalization or (B) qPCR analysis using specific primers for TGF□1, SNAI1, Claudin-2, and E-Cadherin using 18S for normalization. C,D,E: Analysis of alterations in the insulin receptor signaling pathway by PCR and WB, respectively, after PTPRN-depletion in KM12C and KM12SM cell lines. C,D: cDNA synthesized from total RNA from transiently-depleted PTPRN and scrambled control cells after 48h post-transfection was subjected to (C) semi-quantitative RT-PCR analysis using specific primers for IRS1, ERK1, ERK2, AKT1, AKT2, mTOR, FOXO1, AS160, and GSK3α using 18S as control and for normalization or (D) qPCR analysis using specific primers for ERK1, ERK2, AKT1, AKT2, mTOR, FOXO1, and GSK3α using 18S for normalization.. E: Protein expression levels of p-FOXO1/3, GSK3β, p-IRβ, AKT, p-AKT, ERK, p-ERK, and IRS1 in CRC cell lines KM12C and KM12SM transiently transfected with indicated siRNAs for 48h confirmed RT-PCR and/or qPCR results. GAPDH and RhoGDi were used as controls. Red Ponceau staining of each line was used for normalization. A,C,E: Two replicate experiments (1 and 2) were analyzed. Representative images are shown. B,D: Data represent the mean±SD of two experiments. The abundance of each mRNA and protein was quantified by densitometry using Image J.

297x209mm (300 x 300 DPI)

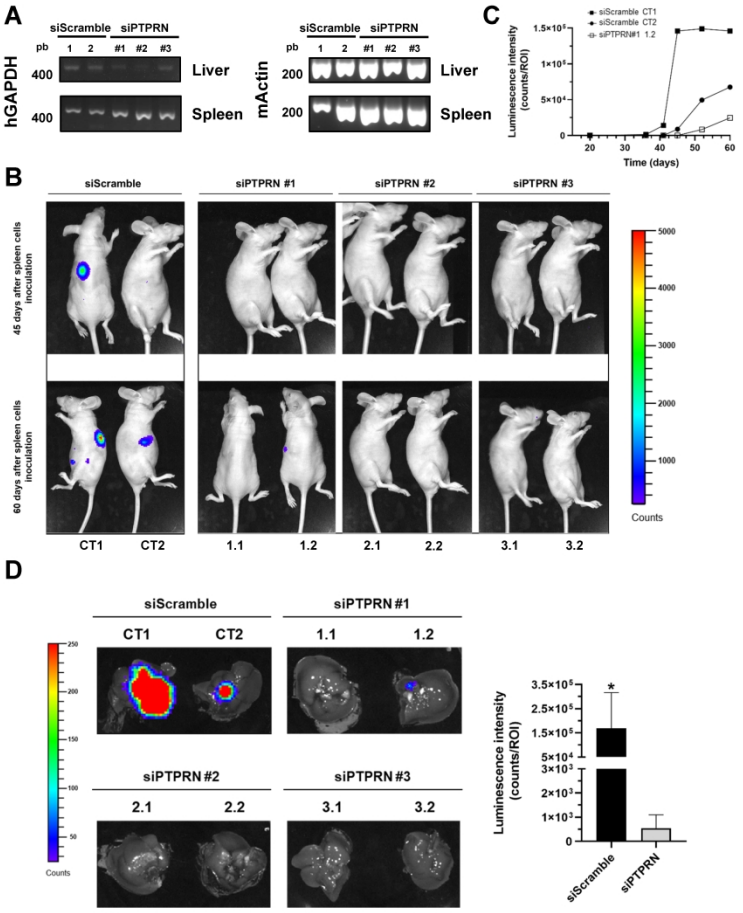

Figure 6

Figure 6-PTPRN depletion decreases liver homing and liver metastasis in KM12SM cells. A: Nude mice intrasplenically inoculated with KM12SM cells transiently transfected with siScramble (n=2) and indicated PTPRN siRNAs (n=1 per PTPRN siRNA) were sacrificed 24 hours after inoculation for analysis of in vivo liver homing. RNA was isolated from the liver and spleen (as control) and directly subjected to RT-PCR to amplify human GAPDH (hGAPDH). Representative experiments out of 2 are shown. Murine β-actin (mβ-actin) was amplified as control. B: Representative images of luminescence intensity of in vivo luciferase activity from mice injected with KM12SM cells transiently transfected with control and PTPRN siRNAs at days 45 and 60 post-intrasplenical inoculation. Mice injected with control cells did show detectable bioluminescence by IVIS analyses, in contrast to mice injected with PTPRN depleted cells (1 out of 6 mice showed detectable luminescence signal). Three mice per group were inoculated, but 1 mouse of each group died prior to metastasis development because of other causes (i.e. after spleen resection, or hemorrhage), and thus n=2 was the final mice number per group. C: Luminescence per indicated mice was represented at each time points. D: At day 60 post-intrasplenical cell inoculation, livers from all control or PTPRN siRNA treated mice were collected and luminescence measured in an IVIS in vivo imaging system. As depicted in the images, 1

out of 6 PTPRN siRNA treated mice showed detectable luminescence, in contrast to the highly measurable luminescence of the two control siRNA mice. Significant luminescence values were observed comparing control and PTPRN siRNA groups, whose luminescence signal was represented by bar graph.

210x297mm (600 x 600 DPI)

ONLINE SUPPLEMENTARY MATERIAL

Cell Lines

KM12SM cells stably expressing firefly luciferase (KM12SM-vLuc cells) were obtained according to established protocols (1). Briefly, firefly luciferase lentiviral particles produced on HEK293T cells transfected with pLV[Exp]-Hygro-EF1A>Luciferase -#85134, Addgene-, psPAX2 -#22036, Addgene- and PM2.G Envelope -#12259, Addgene- were used to infect KM12SM colon cancer liver metastatic cells. After 3-4 weeks of selection with Hygromicin B (100 µg/mL), KM12SM-vLuc cells were grown, maintained in DMEM supplemented with 10% inactivated FBS, L-Glutamine, penicillin/streptomycin and hygromicin B (50 µg/mL) at 37ºC and 5% CO_2, and used in subsequent *in vivo* experiments after transient transfection with PTPRN or control siRNAs.

Gateway Plasmid Construction, Gene Cloning, DNA Preparation and Protein Expression

Sequence-verified, full-length cDNA plasmid containing PTPRN was obtained from the publicly available DNASU Plasmid Repository (https://dnasu.org/DNASU/). The ORF cloned in pDONR221 was transferred by a LR clonase reaction (Invitrogen, Carlsbad, CA) to a pANT7_cHalo vector for *in vitro* protein expression tagged with HaloTag at the C-terminal end (2). All donor and expression plasmids were sequence verified prior to use. To obtain the extra- and intra-cellular domains of PTPRN, PCR amplification of such domains was performed using specific primers with the recombination sites for Gateway cloning (Supplementary Table 2). PCR products were purified and cloned into pDONR221 and subsequently into pANT7_cHalo vector by BP and LR clonase reactions, respectively.

To obtain high-quality supercoiled DNA, plasmids were transformed into TOP10 *E. coli* cells and grown overnight at 37°C in 250 mL Luria Bertani (LB) supplemented with the adequate antibiotic (100 µg/mL ampicillin or 40 µg/mL kanamycin). Plasmid DNA was purified using the NucleoBond® Xtra Midi kit (Macherey-Nagel Inc., Bethlehem, PA). Proteins were expressed using HeLa cell lysates from the 1-Step Human Coupled IVT Kit (Thermo Fisher

Scientific, Waltham, MA) per manufacturer's recommendations to carry out the seroreactivity analyses (3; 4). HaloTag protein was used as negative control of seroreactivity in the assays (3; 4).

EBNA1 ELISA and PTPRN Luminescence Beads Seroreactive Immunoassay

Colorimetric ELISA for EBNA1 antibody determination for the evaluation of the specificity of the study was achieved coating 0.05 µg of EBNA1 protein (kindly provided by Protein Alternatives, S.L.) per well in 50 µl of phosphate-buffer saline solution (PBS) in 96-well transparent plates (Nunc) overnight at 4ºC. Plates were then blocked using a solution of 3% (w/v) skimmed-milk in PBS containing with 0.1% Tween (PBST) for 1 h at 37ºC and then incubated 1 h at 37ºC with 50 µl of the 1:300 diluted plasma samples. After extensive washing with PBST, plates were incubated for 1 h at 37ºC with 50 µl of an HRP-labeled secondary anti-Human IgG antibody (Dako). Lastly, colorimetric signal was developed as previously described (5; 6).

For the luminescence beads seroreactive immunoassays (2-4; 7; 8), PTPRN, ECD or ICD HaloTag fusion proteins were coupled to HaloTag magnetic beads (MBs) by incubating them overnight at 4ºC and 1000 rpm according to the manufacturer's instructions. In total, 0.67 µl of the IVT expression and 0.5 µl of the HaloTag MBs were used per measurement. After extensive washing and removal of non-covalently bound proteins with 0.1 M glycine, pH 2.7, the MBs with the immobilized proteins were blocked with a casein solution during 1 h at room temperature.

To verify covalent protein immobilization, the HaloTag fusion proteins were detected with anti-HaloTag monoclonal antibody diluted 1:1000 (Promega), followed by 1 h of incubation with the HRP-conjugated anti-mouse IgG (Sigma) diluted 1:2500. Alternatively, to evaluate plasma seroreactivity, beads containing the immobilized protein and blocked were placed on black Maxisorp 96-well plates (Nunc) to incubate them overnight with individual plasma samples at indicated dilutions in PBS containing 0.1% Tween 20 (v/v) and 3% BSA (w/v) at 1000 rpm and 4ºC. After washing, a HRP-conjugated anti-human IgG antibody (Dako) diluted

1:10000 in PBS containing 0.1% Tween 20 (v/v) and 3% BSA (w/v) was incubated with the MBs. The MBs signal was developed using 50 µL of SuperSignal ELISA Pico Chemiluminescent Substrate (Pierce, Rockford, IL) for the detection of luminescence on The Spark multimode microplate reader (Tecan Trading AG, Switzerland).

Invasion, Proliferation, and Wound Healing Assays

For Matrigel invasion assays, Transwell chambers (Corning) were coated with 50 µl of a 1:3 dilution in DMEM of 10 mg/ml Matrigel (Sigma). $8x10^4$ KM12 or KM12SM cells in DMEM containing 0.5% BSA (w/v) were seeded on the top Transwell layer, and underneath DMEM, supplemented with 10% FBS was applied. Transwells were then maintained at 37ºC and 5% CO_2 for 22 h. Then, non-invading cells were removed from the upper surface, and cells that migrated through the filter were fixed with 4% paraformaldehyde (Sigma), stained with crystal violet and washed with MilliQ-H_2O, to be counted under a microscope.

For proliferation assays, $5x10^3$ cells were seeded in 100 µl of medium in triplicate into 96-well plates. After 72 h, 50 µl of 3 mg/ml of MTT (3-(4,5-dimethylthiazol-2-yl)-2,5-diphenyltetrazolium bromide) (Sigma) diluted in growth medium was added onto the wells, and the plates were left 1 h at 37ºC. Then, the medium with MTT was carefully removed from the wells, and 50 µl of DMSO was added to disrupt cells and dissolve formazan crystals. After 30 min, the Optical Density (O.D.) at 570 nm was measured using The Spark multimode microplate reader (Tecan Trading AG).

For wound healing, cells were seeded in triplicate in 96-well plates to completely seal the wells. After attachment, a wound was produced and the growth medium replaced. A picture was taken at day 0 and every 12 h for 48 h. The closing area was calculated as pixels using ImageJ and indicated images.

References

1. Brennan TV, Lin L, Huang X, Yang Y: Generation of Luciferase-expressing Tumor Cell Lines. Bio Protoc 2018;8
2. Garranzo-Asensio M, Guzman-Aranguez A, Poves C, Fernandez-Acenero MJ, Torrente-Rodriguez RM, Ruiz-Valdepenas Montiel V, Dominguez G, Frutos LS, Rodriguez N, Villalba M, Pingarron JM, Campuzano S, Barderas R: Toward Liquid Biopsy: Determination of the Humoral Immune Response in Cancer Patients Using HaloTag Fusion Protein-Modified Electrochemical Bioplatforms. Anal Chem 2016;88:12339-12345
3. Garranzo-Asensio M, San Segundo-Acosta P, Poves C, Fernandez-Acenero MJ, Martinez-Useros J, Montero-Calle A, Solis-Fernandez G, Sanchez-Martinez M, Rodriguez N, Ceron MA, Fernandez-Diez S, Dominguez G, de Los Rios V, Pelaez-Garcia A, Guzman-Aranguez A, Barderas R: Identification of tumor-associated antigens with diagnostic ability of colorectal cancer by in-depth immunomic and seroproteomic analysis. Journal of proteomics 2020;214:103635
4. Garranzo-Asensio M, Guzman-Aranguez A, Povedano E, Ruiz-Valdepenas Montiel V, Poves C, Fernandez-Acenero MJ, Montero-Calle A, Solis-Fernandez G, Fernandez-Diez S, Camps J, Arenas M, Rodriguez-Tomas E, Joven J, Sanchez-Martinez M, Rodriguez N, Dominguez G, Yanez-Sedeno P, Pingarron JM, Campuzano S, Barderas R: Multiplexed monitoring of a novel autoantibody diagnostic signature of colorectal cancer using HaloTag technology-based electrochemical immunosensing platform. Theranostics 2020;10:3022-3034
5. Mas S, Boissy P, Monsalve RI, Cuesta-Herranz J, Diaz-Perales A, Fernandez J, Colas C, Rodriguez R, Barderas R, Villalba M: A recombinant Sal k 1 isoform as an alternative to the polymorphic allergen from Salsola kali pollen for allergy diagnosis. Int Arch Allergy Immunol 2015;167:83-93
6. Mas S, Oeo-Santos C, Cuesta-Herranz J, Diaz-Perales A, Colas C, Fernandez J, Barber D, Rodriguez R, de Los Rios V, Barderas R, Villalba M: A relevant IgE-reactive 28kDa protein identified from Salsola kali pollen extract by proteomics is a natural degradation product of an integral 47kDa polygalaturonase. Biochim Biophys Acta Proteins Proteom 2017;1865:1067-1076
7. Montero-Calle A, San Segundo-Acosta P, Garranzo-Asensio M, Rabano A, Barderas R: The Molecular Misreading of APP and UBB Induces a Humoral Immune Response in Alzheimer's Disease Patients with Diagnostic Ability. Mol Neurobiol 2020;57:1009-1020
8. San Segundo-Acosta P, Montero-Calle A, Fuentes M, Rabano A, Villalba M, Barderas R: Identification of Alzheimer's Disease Autoantibodies and Their Target Biomarkers by Phage Microarrays. J Proteome Res 2019;18:2940-2953

Electronic supplementary material Table 1 Clinical and clinicopathological dat

	Code number	Gender*	Age (years)	Type 2 Di Duration (years)**
Control	CT1	F	42	-
	CT2	M	50	-
	CT3	F	24	-
	CT4	F	38	-
	CT5	F	55	-
	CT6	M	44	-
	CT7	F	47	-
	CT8	F	30	-
	CT9	F	46	-
	CT10	F	27	-
Type 2 diabetic patients (T2D)	D1	F	61	5
	D2	F	73	23
	D3	M	69	12
	D4	M	69	17
	D5	M	46	11
	D6	M	61	7
	D7	M	73	28
	D8	M	76	21
	D9	F	54	5
	D10	M	42	2
Colorectal cancer (CRC) patients	CRC1	F	69	-
	CRC2	F	70	-
	CRC3	M	58	-
	CRC4	M	50	-
	CRC5	M	67	-
	CRC6	F	54	-
	CRC7	M	86	-
	CRC8	M	79	-
	CRC9	M	78	-
	CRC10	M	81	-
Type 2 diabetic patients with colorectal cancer (T2D+CRC)	CRC+D1	M	81	13
	CRC+D2	M	72	10
	CRC+D3	M	57	1
	CRC+D4	F	64	2
	CRC+D5	F	61	14
	CRC+D6	M	65	1
	CRC+D7	F	68	2
	CRC+D8	F	69	7

*M, male. F, female.

**Until blood sample collection

*** BMI was only indicated by clinicians when obesity or morbid obesity cofound fa

NA, not available

:a of type 2 diabetic patients with and without colorectal cancer, colorectal cancer patients

iabetes	Medication (treatment)	
Date of diagnosis	T2D	Statin
-	-	
-	-	
-	-	
-	-	
-	-	
-	-	
-	-	
-	-	
-	-	
-	-	
7/4/2013	Metformin. There is a treatment that increases insulin levels, but it is not indicated which is.	Yes
1995	Insulin (Novomix) + metformin + dapagliflozin	Yes
2006	Metformin + dapagliflozin + dulaglutide	Yes
2001	Insulin (Novomix) + metformin + dapagliflozin	-
2007	Insulin (Toujeo + Novorapid) + Meformin + Dapagliflozin	Yes
4/23/2011	Metformin. And there is another treatment that lowers glucose levels, but what it is is not indicated	Yes
1990	Insulin (Toujeo + Humalog) + metformin	Yes
1997	Insulin(glulisine) + vildagliptin	Yes
12/2/2013	Diet	Yes
2016	-	-
-	-	Yes
-	-	Yes
-	-	Yes
-	-	Yes
-	-	-
-	-	Yes
-	-	-
-	-	Yes
-	-	-
-	-	-
01/01/2004	Metformin	-
27/02/2007	Saxagliptin	Yes
10/17/2017	Metformin	Yes
4/10/2015	Metformin + vildagliptin	Yes
8/23/2004	Metformin. There is a treatment that increases insulin levels, but it is not indicated which is.	Yes
08/03/2017	Metformin	Yes
06/04/2016	Metformin	Yes
2/15/2017	Metformin	Yes

ctors were observed in patient or control individuals.

s and healthy individuals as controls.

	TNM staging		
Degree of tumor differentiation	Tumor (T)	Nodes (N)	Metastasis (M)
	-	-	-
	-	-	-
	-	-	-
	-	-	-
	-	-	-
	-	-	-
	-	-	-
	-	-	-
	-	-	-
	-	-	-
	0	-	-
	-	-	-
	-	-	-
	-	-	-
	-	-	-
	0	-	-
	-	-	-
	-	-	-
	0	-	-
	-	-	-
Poorly differentiated	2	N1c	M0
Moderately differentiated	3	N0	M0
Well differentiated	4	N1a	M0
Well differentiated	3	N0	M0
Poorly differentiated	3	N0	M0
Moderately differentiated	3	N0	M0
Well differentiated	2	N0	M0
Poorly differentiated	3	N1c	M0
Moderately differentiated	4	N0	M0
Moderately differentiated	4	N0	M0
Moderately differentiated	2	N0	M0
NA	2	N0	M0
Poorly differentiated	4	N0	M0
Well differentiated	4	N1a	M0
Poorly differentiated	3	N2a	M0
Well differentiated	2	N0	M0
Poorly differentiated	2	N1c	M0
Poorly differentiated	NA	NA	NA

Tumor Location	Lifestyle risk factors and potential and confounding factors (obesity, other diseases…)***
	None
	None
	None
	None
	None
	Obesitiy, BMI: 30
	None
	None
	Obesity, BMI: 33
	None
	Obesity. BMI: 36.52
	None
	None
	None
	None
	Morbid obesity BMI: 43.12, Surgery: Gastric Bypass
	None
	None
	Morbid obesity BMI: 54.78. Surgery: Gastric Bypass
	None
right-sided CRC	None
sigmoid colon	None
left-sided CRC	None
sigmoid colon	None
right-sided CRC	None
sigmoid colon	None
Rectum	None
right-sided CRC	None
sigmoid colon	None
sigmoid colon	None
Rectum	None
sigmoid colon	None
sigmoid colon	None
sigmoid colon	None
sigmoid colon	None
right-sided CRC	None
right-sided CRC	None
NA	None

Electronic supplementary material Table 2 Oligonucleotides used in the study to clone ECD and ICD domains of PTPRN or for amplification of indicated genes.

Gene	Oligonucleotide Forward	Oligonucleotide Reverse	Length (bp)
PTPRN	TGGAGATCCTGGCTGAGCATGT	GGTCACATCAGCCAAAGACAGG	125
E-Cadherin	TGCCCAGAAAATGAAAAAGG	GTGTATGTGGCAATGCGTTC	200
N-Cadherin	ACAGTGGCCACCTACAAAGG	CCGAGATGGGGTTGATAATG	201
SNAI1	GGTTCTTCTGCGCTACTGCT	TAGGGCTGCTGGAAGGTAAA	157
TFGβ1	ACCGGCCTTTCCTGCTTCTCA	CGCCCGGGTTATGCTGGTTGT	288
Claudin2	GCCTCTGGATGGAATGTGCC	GGAGATTGCACTGGATGTCAC	128
ZO-1	CTTACCACACTGTGCGTCCAT	AGGAGTCGGATGATTTTAGAGCA	65
GAPDH	GTCTCCTCTGACTTCAACAGCG	ACCACCCTGTTGCTGTAGCCAA	131
18S	ACCCGTTGAACCCCATTCGTGA	GCCTCACTAAACCATCCAATCGG	159
IRS1	AGTCTGTCGTCCAGTAGCACCA	ACTGGAGCCATACTCATCCGAG	132
PTPRA	GGTGTCTGTAGAGGATGTGACTG	AGTGATGAGGCGCTGTGGCTTT	106
ERK1	TGGCAAGCACTACCTGGATCAG	GCAGAGACTGTAGGTAGTTTCGG	116
ERK2	ACACCAACCTCTCGTACATCGG	TGGCAGTAGGTCTGGTGCTCAA	124
AKT1	TGGACTACCTGCACTCGGAGAA	GTGCCGCAAAAGGTCTTCATGG	154
AKT2	CATCCTCATGGAAGAGATCCGC	GAGGAAGAACCTGTGCTCCATG	148
mTOR	AGCATCGGATGCTTAGGAGTGG	CAGCCAGTCATCTTTGGAGACC	146
FOXO1	CTACGAGTGGATGGTCAAGAGC	CCAGTTCCTTCATTCTGCACACG	138
GSK3α	GCAGATCATGCGTAAGCTGGAC	GGTACACTGTCTCGGGCACATA	128
AS160	ATGAGAGGTCGGCTTGGAAGTG	CGGAATCCTCTTCGGGAAACG	151
hGAPDH (Liver homing analysis)	GGCTGAAGAACGGGAAGCTTGT	CGGCCATCACGCCACAGTTTC	418
m β-Actin (Liver homing analysis)	CATGTACGTAGCCATCCAGGC	CTCTTTGATGTCACGCACGAT	250
ECD cloning*	ggggacaagtttgtacaaaaaagcaggcttcATGGTGCCAAGCCCTGTC	ggggaccactttgtacaagaaagctgggtcGCGCATGGGTGAGGTGCT	-
ICD cloning*	ggggacaagtttgtacaaaaaagcaggcttcATGCGGCAGCATGCGCGG	ggggaccactttgtacaagaaagctgggtcCTGGGGCAGGGCCTTGAG	-

**In upper case, the nucleotide sequence of the genes of interest. In lower case, the nucleotide sequence needed for cloning in the Gateway system.*